Calorimetric Evidence of the Formation of Half-Cylindrical Aggregates of a Cationic Surfactant at the Graphite/Water Interface

Z. Király* and G. H. Findenegg

Technische Universität Berlin, Iwan-N.-Stranski-Institute für Physikalische und Theoretische Chemie, Strasse des 17. Juni 112, 10623 Berlin, Germany

Received: July 8, 1997; In Final Form: December 2, 1997

The adsorption of a cationic surfactant, dodecyltrimethylammonium bromide (C_{12}TAB), from aqueous solutions on graphitized carbon black has been investigated from 288.15 to 318.15 K using a versatile, automated measuring system, which has been designed for the simultaneous measurement of the adsorption isotherm and the calorimetric enthalpies of displacement at the solid/liquid interface. At low concentrations, the surfactant molecules form a flat monolayer on the graphite surface. The enthalpy of monolayer formation is apparently not (or only slightly) dependent on the temperature and is independent of the surface coverage (-61 kJ·mol^{-1}). The adsorption proceeds further as the concentration in the bulk solution is increased to the cmc. In this region, the enthalpy of displacement is again nearly independent of the surface coverage but depends strongly on the temperature: -10.7, -17.5, and -29 kJ·mol^{-1} at 288.15, 298.15, and 318.15 K, respectively. The mechanism of the adsorption and the morphology of the high-density adsorbate structure have been analyzed in terms of the classical reorientation model (reorientation of the adsorbed surfactant molecules from a horizontal to a vertical orientation, accompanied by further adsorption from the bulk solution) and in terms of a recent concept of interfacial aggregation (formation of half-cylindrical surface micelles templated by an epitaxially bound surfactant monolayer). The results of the thermodynamic analysis strongly support the formation of C_{12}TAB half-cylinders at the graphite/water interface.

Introduction

The combination of adsorption isotherms with sorption microcalorimetric data has proved to be a powerful method for screening a variety of surfactant/adsorbent interactions. To date, most calorimetric studies have been directed toward the adsorption from aqueous solutions of nonionic[1−14] and ionic[6,7,15−25] surfactants on *hydrophilic surfaces*, e.g., silica, alumina, clays, etc. It has been established that weakly adsorbed surfactant molecules at low concentrations (low-affinity region of the adsorption isotherm) will induce surface aggregation at higher concentrations as the critical micelle concentration (cmc) in the bulk solution is approached (high-affinity region). Calorimetric studies provided thermodynamic evidence that hydrophobic interactions are the driving force of the aggregative adsorption process, similar to the driving force of micelle formation in the bulk solution. Depending on the systems studied, quasi-spherical micelles, full membrane bilayers, and patchy bilayers have been proposed as the structure of the surface aggregates at surface saturation.

Less attention has been paid to the microcalorimetric investigations of the adsorption from aqueous solutions of nonionic[4,7,26−30] and ionic[7,28,31−33] surfactants on *hydrophobic surfaces*, e.g., activated carbon, carbon black, and graphitized carbon black (gcb). The mechanism of the adsorption and the structure of the adsorption layer are also less well-understood. In contrast with hydrophilic substrates, hydrophobic substrates strongly adsorb surfactants at high dilutions in water. The adsorption proceeds further with increasing concentration until it turns to a plateau and levels off at the cmc. It has been concluded in most adsorption/microcalorimetric studies[26−29,31−33] that initially a horizontally adsorbed monolayer is formed, which is followed by a rearrangement to a vertical orientation providing surface sites for further incoming molecules. This picture implies the formation of a more or less close-packed monolayer at surface saturation, in which the surfactant molecules are oriented with their major axis perpendicular to the surface and their headgroups are exposed to the aqueous phase. For nonionic surfactants, the formation of a horizontally adsorbed bilayer, or even a multilayer, rather than a vertically adsorbed monolayer has also been suggested.[30]

Recently, a novel experimental technique, called noncontact atomic force microscopy (AFM), provided a new insight into the structure of the adsorption layer of ionic surfactants at the solid/liquid interface.[34,35] Direct images of tetradecyltrimethylammonium bromide (C_{14}TAB) and hexadecyltrimethylammonium bromide (C_{16}TAB) surfactants adsorbed on well-defined solid surfaces revealed highly curved structures at concentrations close to the cmc. On hydrophilic surfaces, spherical micelles, or even full cylinders (depending on the surface charge of the substrate), have been identified. On hydrophobic surfaces (graphite, molybdenum disulfide), convincing arguments have been given for the formation of half-cylindrical micelles templated by an epitaxially bound monolayer. Similarly, a recent AFM study on the structure of sodium dodecyl sulfate (SDS) adsorbed to the graphite/solution interface suggested the formation of aligned surface hemicylinders near the bulk cmc.[36] These results challenge current views on how ionic surfactant molecules assemble on hydrophobic substrates. Apart from some electrophoretic mobility measurements[40,42−44] and contact angle measurements,[45] earlier studies of the adsorption of ionic

* Correspondence address: Department of Colloid Chemistry, University of Szeged, Aradi Vt. 1, H-6720 Szeged, Hungary. E-mail: zkiraly@chem.u-szeged.hu.

S1089-5647(97)02218-9 CCC: $15.00
Published on Web 01/27/1998

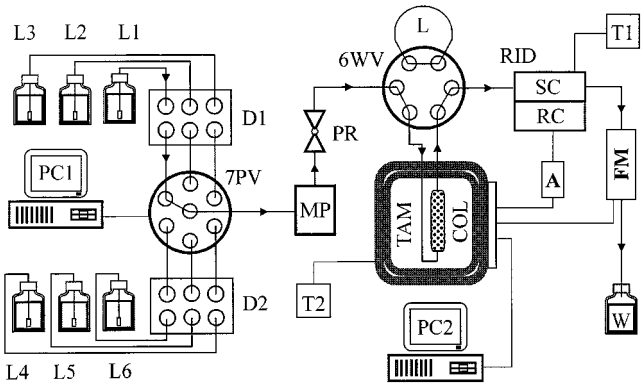

Figure 1. The experimental apparatus designed for the simultaneous measurement of the adsorption isotherm and calorimetric enthalpies of displacement at the solid/solution interface. L1, ..., L6, solutions; D1 and D2, degassers; 7PV, electric seven-port valve; PC1 and PC2, computers; MP, HPLC micropump; PR, pressure regulator; 6WV, six-way valve; L, loop; T1 and T2, thermostats; TAM, thermal activity monitor isotherm microcalorimeter; COL, column; RID, refractive index detector; SC, sample cell; RC, reference cell; A, amplifier; FM, liquid microflowmeter; W, waste.

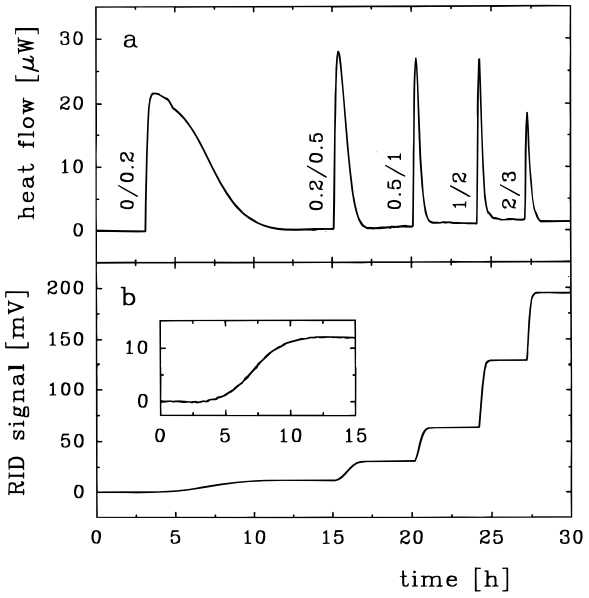

Figure 2. Instrumental response curves of the step-by-step displacement of water by C_{12}TAB on Vulcan 3G at 298.15 K. a, calorimeter signal; b, RID signal (mass of solid, 0.0938 g; flow rate, 117.3 μL·min^{-1}; void volume, 1.5906 cm^3; the concentration increments are indicated in the figure in mmol·dm^{-3}).

surfactants on carbon-type surfaces were mainly restricted to the analysis of the adsorption isotherms[37−45] and the general conclusions, regarding the structure of the adsorption layer at surface saturation, supported the formation of a vertically adsorbed monolayer. The interpretation of the few calorimetric data available for relevant systems led to similar conclusions.[28,31−33]

In this work, we report on the calorimetric investigations of the adsorption of a cationic surfactant, dodecyltrimethylammonium bromide (C_{12}TAB), from aqueous solutions on graphitized carbon black at three different temperatures. The results will be related to the proposed mechanisms for the adsorption of ionic surfactants on hydrophobic substrates. It has recently been criticized that a combination of the adsorption isotherm with the corresponding enthalpy isotherm, measured separately, may cause considerable systematic errors and may lead to false conclusions.[13,14] Owing to technical difficulties, only a few attempts have been reported on the parallel measurements of the two isotherms.[5,6,14,16,17,46] This paper describes a versatile, automated measuring system which allows the simultaneous measurement of the material balance and enthalpy balance of the adsorption at solid/liquid interfaces, providing direct values of differential molar enthalpies related to the adsorption process.

Experimental Section

Materials. C_{12}TAB had a quoted purity of >99% (Aldrich) and was used as received. Stock solutions were prepared by weight and diluted volumetrically with reagent-grade water produced by a Milli-Q filtration system. Vulcan 3 carbon black (supplied by Cabot Corp.) was graphitized at 3000 K for 4 h under an argon atmosphere by Sigri Elektrographit GmbH, Meitingen. The product, Vulcan 3G graphitized carbon black, was treated with *n*-heptane in a Soxhlet extractor for 50 h and dried at 420 K under vacuum. It had a BET surface area of a_s = 68 m^2·g^{-1}.

Equipment. The dynamic technique of frontal analysis[47,48] was applied toward the measurement of the calorimetric enthalpy isotherm of displacement ($\Delta_{21}H$ vs c_1) of water (2) by C_{12}TAB (1) in parallel with the measurement of the volume-reduced adsorption excess isotherm (Γ_1 vs c_1). The experimental apparatus is displayed schematically in Figure 1. Six surfactant solutions [denoted as L1, L2, ..., L6 in Figure 1] with closely spaced concentrations were connected, through six individual channels of two on-line degassers [D1 and D2] (Knauer), to the six outer ports of an electric seven-port valve [7PV] (Knauer). This switching valve was controlled by a computer [PC1]. Switching from one position to another one (say, from L1 to L2) proceeded as the (time) conditions specified in the control program were fulfilled. The central port of the valve was connected to an HPLC micropump [MP] (Knauer) which continuously forwarded the selected solution [L1 in Figure 1] toward the sorption vessel [COL], at a constant flow rate in the range from 6 to 12 mL/h. A back-pressure regulator [PR] (SSI) and a conventional six-way valve [6WV] were inserted between the pump and the vessel. A modified van Os cell[16] was used as the column [COL] (length 26 mm, with an optional inner diameter of 3.1 or 7.5 mm, equipped with two metal filters with a pore width of 7 μm). Before the liquid flow was initiated, the column was loaded with ca. 0.08−0.2 g of gcb pearls and placed inside the measuring block of a TAM isothermal heat-flow microcalorimeter[49] (2277 thermal activity monitor, Thermometric). The solution was pumped through a spiral fine-bore heat-exchange coil just before entering the column. The calorimeter exit port was connected to the sample cell of an on-line differential refractometer (Knauer). From the refractive index detector [RID], the liquid passed up a microflowmeter [FM], (PhaseSep) and finally dropped into a waste container [W]. Teflon, tefzel, or stainless steel capillaries were used for connections throughout. The effective void volume of the system (from the 7PV to the RID) was on the order of 1.5 mL, as obtained from the retention volume of a 2% D_2O solution. The temperature of the column was set to the desired value with an accuracy of 2 × 10^{-4} K; the RID was thermostated at 308.15 ± 0.03 K.

The RID signal was amplified [A in Figure 1] as required to give a maximum resolution of 0.1 mV. The signals from the ancillary equipments were fed through the analogue ports of the calorimeter into the Digitam 3 control software [PC2]. The heat flow across the column and the refractive index of the flowing bulk solution were continuously monitored and recorded (Figure 2). The frequency of data collection was 0.5−0.2 s^{-1},

taking average values over 2−5 counts. Data processing was effected by using either standard or user-defined programs in the Digitam software.

The baseline noise of the calorimeter was to within ±0.05 μW; the baseline noise of the RID was about ±0.05 mV. In general, the baseline drift of the calorimeter was below 0.1 μW/h and the baseline drift of the RID was negligible on the time scale of the experiments. The flow rate, averaged over 40 counts in 10 min, was stable to within ±0.2% over several days.

The flowmeter was calibrated gravimetrically. The clock of the computer used for data collection was calibrated against the clock of the computer used for the control of the electric valve.

Procedures. The progress and the basic principles of the measurements are summarized as follows (see Figure 1). Initially, pure water [L1] is percolated throughout the system until both the calorimeter and the RID display steady baselines. Switching of the electric valve to the next position activates the next (most diluted) solution [L2]. As the solution enters the column (measurement area), a displacement reaction takes place at the interface between the adsorbent and the flowing bulk solution, until the new adsorption equilibrium is established. The material balance and the enthalpy balance of the displacement process can be quantitatively related to the instrumental response curve (Figure 2). The amount adsorbed, $\Delta\Gamma_1$, during a small concentration step, Δc_1, can be calculated from the retention time of the concentration wave.[47,48] The associated (pseudo) differential enthalpy of displacement, $\Delta(\Delta_{21}H)$, can be calculated from the area under the calorimetric peak. After equilibration, the next solution [L3] is selected by the electric valve, etc. The step-by-step sequence of L1, L2, ..., L6 (adsorption path) is then followed in the reverse direction (step-by-step desorption), and finally, the first set of measurements is completed by returning to solution L6. At this stage, the data collection is suspended, the 6WV is switched manually from the "column" position to the "load" position, and the first set of five solutions is carefully replaced by the second set of five solutions (say, with increasing concentrations from L5 to L1). During this flushing/reloading procedure, there is no liquid flow in the sorption vessel (the liquid is pumped to the waste container through the loop, L) and the column is unaffected by the installation of the new solutions. In the second set of the measurement, the 6WV is switched back to the column position and the liquid flow is restarted by using L6 as the first solution. The adsorption experiment proceeds step-by-step toward L1.

For the present system, a complete cumulative experiment consisted of 3 sets of measurements (12−14 different concentrations) at each temperature (288.15, 298.15, and 318.15 K). The step-by-step data were gathered and summed over the concentration range of interest to construct the cumulative adsorption isotherm Γ_1 vs c_1 and the cumulative (or integral) enthalpy isotherm of displacement $\Delta_{21}H$ vs c_1. The standard deviation of a single step of the step-by-step adsorption experiment was 2.7% on average, while for calorimetry it was about 2.2%. This accuracy provides more reliable differential molar enthalpy data, calculated directly as $\Delta_{21}h_1 = \Delta(\Delta_{21}H)/\Delta\Gamma_1$ for each step, than a combination of separately measured adsorption and calorimetric enthalpy isotherms.

Besides the step-by-step method (L1, L2, ..., L6, L5, ..., L1), we also employed the single-step method (described by the sequence L1, L2, L1, L3, ..., L1, L6, L1), i.e., starting from or returning to the same solution for each step. However, for this method, we experienced an increased scatter in the retention time data. This is attributed to a decreasing retention volume/dead volume ratio as the concentration differences are increased. On the other hand, the application of high-concentration steps through a less tightly packed column (as compared with a conventional HPLC column) reduces the efficiency of the separation and may lead to the appearance of some nonequilibrium effects (back-mixing, channeling, and other complexities[47,50,51]). Further, the heat of mixing at the interface between the replacing and replaced solutions in the column may superimpose on the enthalpy of displacement.[50,51]

Some kinetic hindrances (appearing as an elongated breakthrough curve and a tailing of the calorimetric peak) were observed for the last two desorption steps on returning to pure water. Otherwise, the repeated experiments and the adsorption−desorption cycles indicated completely reversible displacement processes at each temperature. It should be noted that for a nonreversible adsorption/displacement process, fresh solid samples may be required to complete the experiment.

The measuring system reported in this work provides high accuracy and reproducibility. The excellent stability of the system and the automated design allows essentially nonstop measurements, with occasional breaks for changing the solution samples, the column packing, or the temperature.

Thermodynamic Considerations

Displacement of solvent (2) by solute (1) at the solid/liquid interface can be represented by the stoichiometric equation[48,52,53]

$$(1)^{l} + r\,(2)^{s} = (1)^{s} + r\,(2)^{l} \qquad (1)$$

where the superscripts s and l refer to the adsorption layer and the bulk liquid phase, respectively, and r is the amount of solvent displaced by 1 mol of solute at concentration c_1. We recall the definition of the differential molar enthalpy of displacement, $\Delta_{21}h_1$, as the difference between the partial molar enthalpies (h_i) of the two components in the adsorption layer and the equilibrium bulk solution:[48,52−54]

$$\Delta_{21}h_1 = \left[\frac{\partial(\Delta_{21}H)}{\partial\Gamma_1^{s}}\right]_{T,p,a_s} = (h_1^{s} - h_1^{l}) - r(h_2^{s} - h_2^{l}) \quad (2)$$

where $\Delta_{21}H$ is the integral enthalpy of displacement and Γ_1^s is the amount of solute actually present in the adsorption layer. In the case of dilute solutions and preferential adsorption of the solute, the real amount adsorbed is practically equal to the surface excess concentration; i.e., $\Gamma_1^s = \Gamma_1$.[55] If the flow replacement experiment involves small concentration increments, $\Delta_{21}H$ is equal to the cumulative enthalpy of displacement, while $\Delta_{21}h_1$ may be approximated by the pseudo-differential enthalpy of displacement, $\Delta(\Delta_{21}H)/\Delta\Gamma_1$. It should be emphasized that the above definition of $\Delta_{21}h_1$ implies that the reference state of the displacement process is the equilibrium bulk solution, rather than pure water.[53,54] This statement is of great importance, because thermodynamic quantities of surfactant solutions, like the enthalpy and the heat capacity of micelle formation, are related to either the infinite dilution state or the surfactant solution at the cmc, allowing a direct comparison between thermodynamic quantities of surfactant aggregations in the bulk solution and at the solid/liquid interface. For further details about displacement thermodynamic quantities, we refer to earlier works.[52−54]

Results

The adsorption isotherms of C_{12}TAB(1)−water(2)/gcb at 288.15, 298.15, and 318.15 K are shown in Figure 3. Although

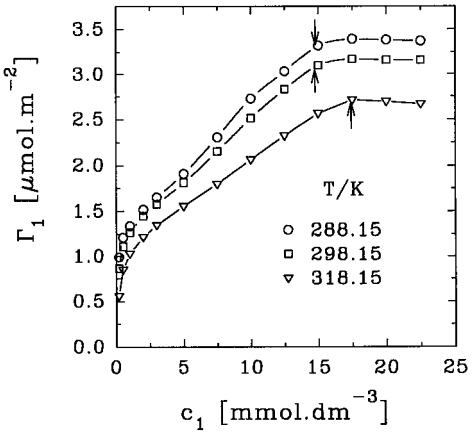

Figure 3. Cumulative adsorption isotherms of C_{12}TAB (1)−water (2)/Vulcan 3G at different temperatures. The arrows indicate cmc values.

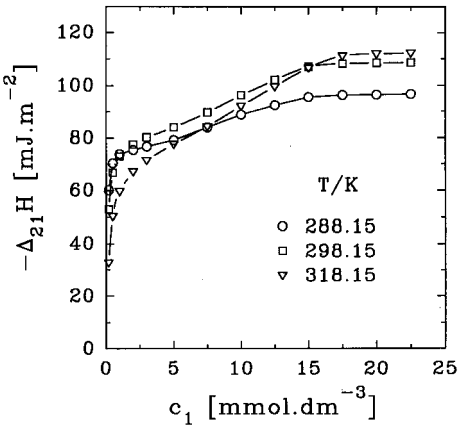

Figure 4. Cumulative enthalpies of the displacement of water (2) by C_{12}TAB (1) on Vulcan 3G at different temperatures.

the extent of adsorption is decreasing with increasing temperature (normal temperature effect), the characteristic features of all three isotherms are very similar. A sudden increase of the adsorption isotherm turns to a knee which is followed by a more or less pronounced point of inflection. The adsorption continues to increase, and the isotherm goes through a second point of inflection (which can hardly be seen in the figure) until it turns to a plateau. A minor decrease in the adsorption can be observed beyond the cmc. The complex shape of the adsorption isotherm will be analyzed in details in a forthcoming publication, in which a different chromatographic technique has been applied.[56] This method, called the elution on the plateau, is very sensitive to the fine structure of the isotherm, because the slope of the isotherm, $d\Gamma_1/dc_1$, is directly measured as a function of c_1.

The integral enthalpy isotherms of displacement of water by C_{12}TAB, displayed in Figure 4, are similar in shape to the corresponding adsorption isotherms. It is remarkable that while at low concentrations the displacement process becomes less exothermic with increasing temperature (at least on the concentration scale), the opposite holds true at higher concentrations. This observation suggests a two-stage adsorption process, the first stage of which is more exothermic than the second.

The differential molar enthalpies of displacement are plotted against the surface concentration in Figure 5. Two regions, referred to as I and II, can be distinguished in this representation, which are linked together by a transition zone. In region I, the displacement of water by C_{12}TAB is strongly exothermic and is *apparently* independent of surface coverage up to the transition zone. Unfortunately, there are insufficient experi-

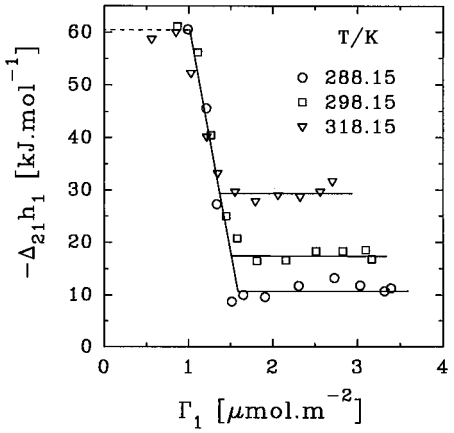

Figure 5. Differential molar enthalpies of the displacement of water (2) by C_{12}TAB (1) on Vulcan 3G at different temperatures (lines are drawn to guide the reader's eye).

mental data at low surface coverages (<1 μmol·m^{-2}), because the surfactant adsorbs strongly on gcb, even in highly water-diluted solutions, and the detection of very low concentrations (<0.2 mM) was limited by the sensitivity of the refractometer. Nevertheless, the experimental data available in this region, and similar studies on C_6-, C_8-, and C_{10}TAB,[57] for which more adsorption and enthalpy data were obtained at low surface coverages, strongly support the conclusion concerning the constancy of $\Delta_{21}h_1^{I}$. The implication of this conclusion is that the adsorption layer behaves ideally in region I. Further inspection of Figure 5 suggests that $\Delta_{21}h_1^{I}$ is independent (or nearly independent) of temperature. Beyond the transition zone, the enthalpy of the formation of the adsorption layer in region II, $\Delta_{21}h_1^{II}$, becomes independent of surface coverage, or weakly decreases in magnitude. Region II is appreciably less exothermic than region I. It is peculiar that $-\Delta_{21}h_1^{II}$ increases in magnitude as the temperature is increased. An average value of ca. −61 kJ·mol^{-1} can be ascribed for $\Delta_{21}h_1^{I}$, independent of temperature, while $\Delta_{21}h_1^{II}$ is found to be −10.7, −17.5, and −29 kJ·mol^{-1} at 288.15, 298.15, and 318.15 K, respectively (Table 1). The transition region is smeared out over a range of surface coverage, which implies some overlapping between the two successive stages of the adsorption. The nominal boundary between I and II can be localized by taking the half-width position of the transition regime. A careful regression analysis was used for the determination of the characteristic surface concentrations, Γ_1^{I}, which can be ascribed to the completion of the displacement process in region I. The plateau values of the adsorption isotherms, Γ_1^{II}, are regarded as further characteristic surface concentrations, being related to the completion of the displacement process in region II. The following values were obtained: 1.32, 1.28, and 1.20 μmol·m^{-2} for the adsorption in region I and 3.39, 3.17, and 2.71 μmol·m^{-2} in region II at 288.15, 298.15, and 318.15 K, respectively (Table 1). It should be noted that while Γ_1^{II} is taken as the plateau value of the adsorption isotherm, the determination of Γ_1^{I} requires the knowledge of both the adsorption isotherm and the calorimetric enthalpy isotherm of displacement. Γ_1^{I} is positioned somewhere at the knee of the adsorption isotherm, before the first point of inflection is reached.

Discussion

Adsorption Process in Region I. We correlate the displacement process in region I with the formation of an epitaxially bound monolayer of C_{12}TAB molecules in a head-to-head and tail-to-tail arrangement. Such a structure has been first proposed

TABLE 1: Thermodynamic Parameters of the Aggregation and Adsorption of C_{12}TAB in Aqueous Bulk Solutions and at the Water/Gcb Interface[a]

T, K	cmc(aq), mM	cmc(el), mM	Γ_1^{I}, μmol·m^{-2}	Γ_1^{II}, μmol·m^{-2}	n_{hc}^{II}	n_{sp}(aq)
288.15	14.7	12.3	1.32	3.39	5.14	67
298.15	14.6	13.0	1.28	3.17	4.95	63
318.15	17.5	13.5	1.20	2.71	4.52	53
T, K	$\Delta_{mic}H^{\infty}$(aq),[b] kJ·mol^{-1}	$\Delta_{mic}H^{\infty}$(el),[c] kJ·mol^{-1}	$\Delta_{21}h_1^{I}$, kJ·mol^{-1}	$\Delta_{21}h_1^{II}$, kJ·mol^{-1}	$\Delta_{re}H$, kJ·mol^{-1}	$\Delta_{va}H$, kJ·mol^{-1}
288.15	2.86	0.30	≈−61	−10.7 ± 0.9	30.2	−30.8
298.15	−1.20	−4.05	≈−61	−17.5 ± 0.9	26.1	−34.9
318.15	−9.31	−11.55	≈−61	−29.0 ± 0.6	19.2	−41.8
Δc_p, J·mol^{-1}·K^{-1}	−406[d]	−392[c]	≈0	−605	−364	−364

[a] cmc(aq): critical micelle concentration in aqueous bulk solution.[71] cmc(el): critical micelle concentration in aqueous bulk solution in the presence of electrolyte (NaBr:C_{12}TAB = 1:1).[73] Γ_1^{I}: maximum value of the adsorbed amount of C_{12}TAB on gcb in adsorption region I (monolayer capacity). Γ_1^{II}: maximum value of the adsorbed amount of C_{12}TAB on gcb in adsorption region I + II (adsorption plateau). n_{hc}^{II}: number of surfactant molecules in a single sheet of half-cylindrical surface micelles of C_{12}TAB on gcb at the plateau, calculated as $2\Gamma_1^{II}/\Gamma_1^{I}$. n_{sp}(aq): aggregation number of spherical micelles in aqueous bulk solution.[70] $\Delta_{mic}H^{\infty}$(aq): enthalpy of formation of spherical micelles in aqueous bulk solution (infinite dilution reference).[71] $\Delta_{mic}H^{\infty}$(el): enthalpy of formation of spherical micelles in aqueous bulk solution in the presence of electrolyte (NaBr:C_{12}TAB = 1:1, infinite dilution reference).[73] $\Delta_{21}h_1^{I}$: differential molar enthalpy of displacement of water (2) by C_{12}TAB (1) on gcb in adsorption region I; reference state, equilibrium bulk solution. $\Delta_{21}h_1^{II}$: differential molar enthalpy of displacement of water (2) by C_{12}TAB (1) on gcb in adsorption region II; reference state, equilibrium bulk solution. $\Delta_{re}H$: enthalpy of reorientation from a horizontal to a semivertical orientation in adsorption region II, according to the reorientation model. $\Delta_{va}H$: enthalpy of adsorption in a semivertical orientation in adsorption region II, according to the reorientation model. Δc_p: molar heat capacity. [b] Fitted data, Table 6 in ref 71. [c] Fitted data, Table 7 in ref 73. [d] Reference 72.

by Manne et al., who investigated the morphology of C_{14}TAB and C_{16}TAB surfactants adsorbed at the graphite/water interface by atomic force microscopy (AFM).[34,35] The analysis of the striped AFM patterns revealed that the tails of the surfactant molecules are oriented parallel to the three equivalent symmetry axes of the graphite basal plane, giving rise to the formation of organized two-dimensional domains in the three major orientations. The hydrophobic attraction between long-chain alkane molecules and the graphite surface is well-established experimentally.[52,58−60] However, the formation of a surfactant monolayer with ionic headgroups neighboring each other is not quite straightforward. The arguments of Manne et al.,[34,35] which account for this kind of orientation, are summarized as follows. First, the structures of bulk crystalline C_xTABs also imply a head-to-head packing,[61] with a long axis periodicity close to the regular spacings observed in C_xTAB monolayers on graphite. Second, a partial association of the adsorbed alkylammonium ions with bromide ions can stabilize the headgroups against electrostatic repulsion, similar to C_xTAB micelles, where ca. 75% of the surfactant molecules in the micelles are charge-neutralized by bound counterions.[62] Third, electrostatic repulsion between neighboring headgroups may be partially counterbalanced by the adsorption of the methyl groups of the ammonium head. Fourth, the graphite surface possesses a moderate electrical conductivity which may also contribute, via attractive forces toward the charged headgroups, to the stabilization of a head-to-head arrangement. Manne et al. observed periodicities about twice the surfactant length. Therefore, the idea of an alternating head-to-tail packing in a monolayer of horizontally adsorbed surfactant molecules, as the reorientation model suggested,[32,33,45] is not supported by these observations.

The plane of the carbon skeleton of alkyl derivatives can be oriented either perpendicular to or parallel with the substrate surface. In situ scanning tunneling microscopy (STM) studies revealed that if the headgroup requires more space (as in the present case), then the parallel orientation is preferred.[59] Due to electrostatic repulsion between the neighboring headgroups, the formation of a perfectly close-packed monolayer, as occurs for *n*-alkanes at the liquid/graphite interface,[52,58−60] is unlikely for C_xTABs. The positions of the carbon atoms in an alkane chain closely match those of the graphite surface. Groszek proposed a geometric model in which each methylene group occupies one hexagon (5.24 nm^2), while the methyl group occupies two hexagons on the graphite basal plane.[52,60] Assuming that the occupation area of the trimethylammonium head is 5 hexagons (1 hexagon for the nitrogen atom and 2 × 2 hexagons for 2 methyl groups, the third being exposed to the aqueous phase), the geometric model would give a value of $\Gamma_1^{I} = 1.76$ μmol·m^{-2} for C_{12}TAB in a close-packed monolayer. A comparison with $\Gamma_1^{I} = 1.28$ μmol·m^{-2}, obtained in the present analysis at 298.15 K, suggests that only 73% of the gcb surface is covered by C_{12}TAB molecules. The real surface coverage is presumably somewhat higher since, in general, the geometric model provides an overestimate of the monomolecular adsorption capacities due to some mismatch between the flat-lying alkyl skeleton and the graphite lattice.[52,59] The length of an extended C_xTAB molecule in the all-trans conformation of the alkyl chain is given by

$$l(\mathrm{C}_x\mathrm{TAB}) = 0.245\left(\frac{x}{2} - 1\right) + r_{\mathrm{Me}} + r_{\mathrm{N-Me}} \qquad (3)$$

with the van der Waals radii of the methyl (r_{Me} = 0.20 nm) and the trimethylammonium (r_{N-Me} = 0.35 nm) end groups.[63] This formula yields l = 1.78 nm for C_{12}TAB in a zigzag conformation. On the assumption that the incomplete C_{12}TAB monolayer is predominantly attributed to head-to-head repulsion (which is more pronounced for the less hydrophobic shorter chain homologues) and using the value of 73% as the surface coverage in an ordered array, a periodicity of 4.9 nm is predicted for a head-to-head, tail-to-tail arrangement. This value can be compared with the spacings of 4.7 and 4.2 nm for C_{14}TAB and C_{16}TAB, respectively, obtained from AFM analysis.[34,35] The free surface sites which are not covered by adsorbed organic cations may be localized to narrow stripes between neighboring rows of headgroups where the counter bromide ions are accommodated. The absence of close-packing may be partly due to the different diameters of the alkyl chain and the headgroup, the latter being larger than the former. An inclination of the tails on the surface,[59] relative to the observed rows of headgroups, would favor a closer packing of the longer chain homologue. Such a tilted orientation can also explain that the

spacing between the stripes on the AFM images was found to be smaller for C_{16}TAB than for C_{14}TAB.

A further question arises, whether the adsorption is driven by the registry between the carbon lattices of adsorbate and substrate or by a two-dimensional crystallization of the adsorbate on the substrate, independent of the substrate lattice.[35,59] We propose that the surfactant molecules form tiny islands on the graphite surface at the very early stage of the adsorption process, serving as nuclei for a two-dimensional growth at the expense of surface-bound water, as the adsorption proceeds. Such a mechanism is consistent with the formation of two-dimensional ordered domains, observed by AFM and STM, and with an ideal adsorption layer, as suggested by the constancy of $\Delta_{21}h_1^{\mathrm{I}}$ in region I. The high negative value of $\Delta_{21}h_1^{\mathrm{I}} = -61$ kJ·mol^{-1} further supports the formation of a strongly bound, solidlike ordered monolayer structure. For a comparison, the heat of solution of crystalline C_{12}TAB at infinite dilution in water, as interpolated from the data available for C_{10}TAB and C_{16}TAB at 298.15 K, is ca. 43 kJ·mol^{-1}.[64,65] Further, the enthalpy of transition of C_{12}TAB from the solid phase to a liquidlike mesophase (some 150 K below the melting temperature) is ca. 44 kJ·mol^{-1}.[61]

Adsorption Process in Region II. The headgroup of the adsorbed surfactant molecules must be exposed to the aqueous phase in the high-density adsorption regime. In fact, only such an orientation can explain the low contact angles, the high electrophoretic mobility, and the related stability of carbon black particles dispersed in aqueous solutions of ionic surfactants.[40,42−45] Both the formation of surface half-cylinders and a vertically oriented monolayer structure comply with these experimental observations. With the aim of finding thermodynamic arguments for (or against) these models, for region II, we discuss our results in terms of the two models separately.

Half-Cylindrical Model. We correlate the displacement process in region II with the formation of half-cylindrical C_{12}TAB micelles induced by the preadsorbed monolayer. For C_{14}TAB and C_{16}TAB, Manne et al. postulated that a horizontally adsorbed ordered monolayer serves as a template for surface micellization as the concentration in the bulk solution is increased.[34,35] These authors argued that the formation of half-cylinders on the graphite surface represents a compromise between two opposing forces: surfactant molecules tend to form curved structures because of intermolecular attraction, whereas the surface pulls them toward a flat arrangement for maximum interfacial contact. A half-cylinder may be regarded as an intermediate between a naturally curved structure and a flat adsorption layer.

It has been established that the formation of rodlike micelles of C_xTAB surfactants can be induced in the bulk solution upon the addition of electrolytes[66−68] or, in the absence of electrolyte, by increasing the surfactant concentration or decreasing the temperature.[69] Since the formation of rodlike micelles can be induced under various conditions, an epitaxially bound surfactant monolayer may also serve as a template for half-cylindrical micelles. Assuming that the adsorption in region II for the present system correlates with this model, we can estimate the number of C_{12}TAB molecules, n_{hc}, in a single layer perpendicular to the major axis of a half-cylinder:

$$n_{\mathrm{hc}} = 2\Gamma_1^{\mathrm{II}}/\Gamma_1^{\mathrm{I}} \qquad (4)$$

The results of the calculation are listed in Table 1. It appears that the number of molecules in a unit sheet of the C_{12}TAB half-cylinders is $n_{\mathrm{hc}} = 5$ on average. The scatter around a value of 5 may arise in part from the cumulative error involved in

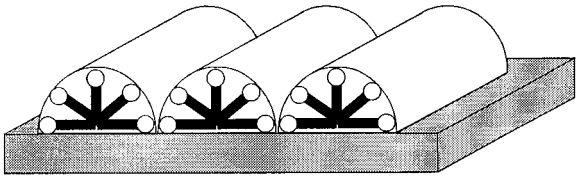

Figure 6. Proposed structure of C_{12}TAB half-cylindrical hemimicelles at the graphite/water interface (schematic).

Γ_1^{II} as well as from some uncertainties in specifying the position of Γ_1^{I}. In the temperature range investigated in this work, n_{hc} seems to slightly decrease with increasing temperature, similar to the aggregation number, n_{sp}, of spherical C_{12}TAB micelles in the bulk solution[70] (Table 1). The number of molecules in a disklike layer of cylindrical micelles of C_{16}TAB, C_{12}DAB (dodecyldimethylammonium bromide), and C_{12}TAC (dodecyldimethylammonium chloride) has been reported to be 17, 16, and 13, respectively.[68] Taking into consideration the geometric constraint which is imposed on the micelle formation at a plane surface, $n_{\mathrm{hc}} = 5$ seems to be a reasonable value for a C_{12}TAB surface half-cylinder. The proposed structure of the surface aggregates is sketched in Figure 6. While the template molecules are strongly bound to the surface, the remaining of the C_{12}TAB surface micelles are more mobile. This may be inferred from the low value of n_{hc} and from a comparison of the values of $\Delta_{21}h_1$ in regions I and II (Table 1). The weak increase in $-\Delta_{21}h_1^{\mathrm{II}}$ with increasing adsorbate density, suggested by the experimental data in Figure 5, and the sigmoidal shape of the adsorption isotherm in region II (see Figure 3) may also be related to the cooperative mechanism of the surface aggregation process. $\Delta_{21}h_1^{\mathrm{II}}$ can be further compared with the corresponding enthalpies of spherical micelle formation, both in the absence ($\Delta_{\mathrm{mic}}H^{\infty}$(aq))[71,72] and in the presence ($\Delta_{\mathrm{mic}}H^{\infty}$(el))[73] of added electrolyte (Table 1). At each temperature, $\Delta_{21}h_1^{\mathrm{II}}$ is more negative than $\Delta_{\mathrm{mic}}H^{\infty}$. A detailed calorimetric study on the micellar properties of aqueous SDS solutions indicated that the transition from spherical to cylindrical micelles (in the presence of NaCl) is, in fact, an exothermic process.[74,75] To our knowledge, no similar studies have been reported for C_xTAB or other relevant surfactants. (It may be noted that in a titration calorimetric study of water by a micellar solution of C_{16}TAB,[65] the authors observed an anomaly on the titration curve and $\Delta_{\mathrm{mic}}H$ at 298 K was found to be 2 kJ·mol^{-1} more exothermic than the $\Delta_{\mathrm{mic}}H$ obtained in other calorimetric studies.[71,76] A comparison of the cmc of C_{16}TAB cylinders (ca. 5 wt %[69]) with the concentration of the titrant in the aforementioned calorimetric experiment (17 wt %) shows that the titration experiment was performed by using a cylindrical rather than a spherical micellar solution. If so, the sphere-to-rod transition for C_{16}TAB is also an exothermic process.) The strong temperature dependence of $\Delta_{21}h_1^{\mathrm{II}}$ compares well with the strong temperature dependence of $\Delta_{\mathrm{mic}}H^{\infty}$. In view of the analogy between the displacement process in region II and micelle formation in the bulk solution, the corresponding molar enthalpies are plotted against temperature in Figure 7. For a further comparison, enthalpy data relating to the aggregative adsorption (or the formation of quasi-spherical surface micelles) of C_{12}TAB at the hydrophilic silica/water interface[10] are also indicated in the figure. Although in this set of measurements the adsorption isotherms and the enthalpies of displacement were measured separately, which might imply a higher experimental error, it does not affect the general conclusion which can be drawn from Figure 7. The similar temperature dependence, depicted from the four curves, indicates that micelle formation in the bulk solution and surface micellization at the solid/solution interface are very similar

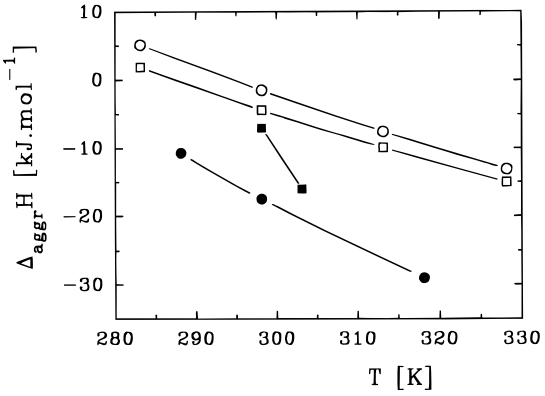

Figure 7. Molar enthalpies of the aggregate formation of C_{12}TAB in various environments plotted against temperature: (○) in aqueous solution [ref 71]; (□) in aqueous solution in the presence of electrolyte NaBr:C_{12}TAB = 1:1 [ref 73]; (■) at the hydrophilic silica/water interface [ref 10]; (●) at the graphite/water interface [this work].

phenomena, originating from the driving force of hydrophobic interactions. It appears that the respective molar enthalpies $\Delta_{mic}H$ or $\Delta_{21}h_1^{II}$ become more exothermic in the order aqueous solution < dilute aqueous electrolyte solution < silca/water interface < gcb/water interface. This trend may be related to the extent of the perturbation of the aggregates in a particular micellar environment relative to a spherical C_{12}TAB micelle in aqueous solution. It is interesting to note that, depending on the number of active surface sites on the substrate, Manne et al. observed either isolated or interconnected spherical aggregates of C_{14}TAB at the silica/aqueous solution interface.[35] Further, in our recent calorimetric study on the adsorption of *n*-octyl tetraoxyethylene glycol monoether and *n*-octyl monoglucoside nonionic surfactants from aqueous solutions on hydrophilic silica, we found that $\Delta_{21}h_1^{II}$ is nearly equal to $\Delta_{mic}H$, suggesting that the structure of the surface aggregates is similar to the structure of the micelles in the bulk solution in that case.[14] For the present system, however, $\Delta_{21}h_1^{II}$ is significantly more negative than $\Delta_{mic}H$, but the corresponding heat capacities are remarkably similar (Table 1). In the calorimetric study of aqueous micellar solutions of SDS (referred to earlier in this section), evidence has been given that while the sphere-to-rod transition is an exothermic process, there is only a small heat-capacity change associated with this process; i.e., the temperature dependence of the enthalpy of formation of spherical micelles is similar to that of rodlike micelles.[75] Considering that half-cylindrical SDS aggregates may exist on graphite,[36] this finding may be regarded as a further, indirect argument for the formation of C_{12}TAB half-cylinders in our system.

Reorientation Model. Although the formation of a vertically oriented monolayer is not justified by the aforementioned AFM study, since structuring should not be visible on the AFM patterns in this case, we focus our attention here on the thermodynamic aspects of this model. On the assumption that all C_{12}TAB molecules were adsorbed perpendicular to the graphite surface at the plateau of the adsorption isotherm, the limiting value of the area per surfactant molecule can readily be calculated from Γ_1^{II} to give 0.49, 0.53, and 0.62 nm^2/molecule at 288.15, 298.15, and 318.15 K, respectively. An increase in headgroup repulsion between neighboring adsorbate molecules, and/or an increase in the mobility of the alkyl chains as the temperature is increased, can well account for these apparent cross-sectional molecular areas. It may be doubtful, however, to arrive at the right conclusions regarding the structure of the adsorption layer which relies solely on the analysis of the adsorption isotherm.

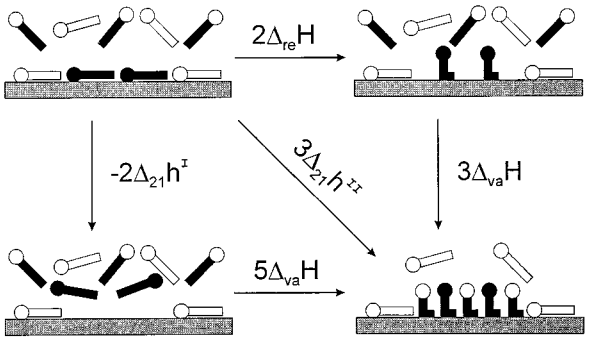

Figure 8. Proposed enthalpy balance for a thermodynamic analysis of the reorientation model (schematic). $\Delta_{re}H$, molar enthalpy of reorientation from a horizontal to a (partially) vertical orientation; $\Delta_{va}H$, molar enthalpy of adsorption in a (partially) vertical orientation; $\Delta_{21}h^{I}$ and $\Delta_{21}h^{II}$, differential molar enthalpies of displacement in the low- (I) and high-density (II) adsorbate regions, respectively. The stoichiometry roughly scales for C_{12}TAB at the graphite/water interface (see text). The cycles comply with Hess' law.

As mentioned before, the large exothermic enthalpy of displacement in adsorption region I (-61 kJ·mol^{-1}) indicates a stable, strongly bound adsorbate structure at the graphite surface. Even irreversible adsorption has been experienced for C_{16}TAB[42] and some nonionic surfactants[30] on carbon-type surfaces. Although the flow sorption experiment proved to be reversible in the present case, heavy smearing of the concentration wave and strongly elongated calorimetric peaks were observed during the desorption experiments below a concentration of 0.5 mM. These observations strongly indicate that a reorientation (partial desorption) of the horizontally adsorbed C_{12}TAB molecules is unlikely to occur. Supposing it does occur, the enthalpy of reorientation, $\Delta_{re}H$, and the enthalpy of further adsorption in a vertical (or some intermediate between vertical and horizontal) orientation, $\Delta_{va}H$, can be estimated from the adsorption isotherms and the calorimetric data. If one preadsorbed (host) molecule is lifted away from the surface, providing room for *n* further incoming (guest) molecules, and assuming, that the host and guest molecules are indistinguishable in the new adsorbed state (i.e., they have an identical number of surface contacts, occupational area, configuration, etc.), then $\Delta_{va}H = \Delta_{21}h_1^{I} + \Delta_{re}H$ and $\Delta_{21}h_1^{II} = \Delta_{re}H/n + \Delta_{va}H$ so that

$$\Delta_{re}H = \frac{n}{n+1}[\Delta_{21}h_1^{II} - \Delta_{21}h_1^{I}] \quad (5)$$

$$\Delta_{va}H = \frac{n\Delta_{21}h_1^{II} + \Delta_{21}h_1^{I}}{n+1} \quad (6)$$

n is related to the surface concentrations at the monolayer and the plateau as $n = \Gamma_1^{II}/\Gamma_1^{I} - 1$. The present results yield $n = 1.5$ on average. Physically, this is equivalent to the reorientation of two host molecules giving rise to the adsorption of three guest molecules. The reorientation scheme is shown in Figure 8. The reorientation of one host molecule accompanied by the adsorption of *n* guest molecules is equivalent to the hypothetical process of the transfer of one horizontally adsorbed C_{12}TAB molecule, away from the surface into the bulk solution, and then transferring $n + 1$ surfactant molecules from the bulk liquid phase onto the solid surface in a vertical (or some intermediate) orientation. This hypothetical process is also indicated in Figure 8. The cycles in the figure comply with Hess' law. It may be expected that while the reorientation of the host molecules is an endothermic process, the adsorption of the guest molecules is an exothermic process. Indeed, application of eqs 5 and 6

yields 30.2, 26.1, and 19 kJ·mol^{-1} for $\Delta_{re}H$ and −30.8, −34.9, and −41.8 kJ·mol^{-1} for $\Delta_{va}H$, at 288.15, 298.15, and 318.15 K, respectively (Table 1). However, the estimated values for $\Delta_{va}H$ are more negative than what one might expect for a partial adsorption of the C_{12} chains, recalling that an experimental value of $\Delta_{21}h_1^{I} = -61$ kJ·mol^{-1} was obtained for surfactant molecules lying flat on the surface. By using an equivalent surface area, rather than the molecular occupational areas in the two orientations, we obtain $(n + 1)\Delta_{va}H/\Delta_{21}h_1^{I} > 1$ by a factor in the range from 1.26 to 1.71. In other words, if the adsorption per unit segment in a semivertical orientation were energetically favored to the adsorption per unit segment in a horizontal orientation, the surfactant molecules would be adsorbed perpendicular rather than parallel to the surface even in region I. Further, the estimated values of $\Delta_{va}H$ imply that $\Delta_{va}H$ is *strongly* temperature dependent (see Δc_p data in Table 1). This finding contradicts the *apparent* temperature independence of the displacement process in region I, since the associated heat effect originates from a direct contact with the graphite surface in either case. The negative temperature dependence of $\Delta_{va}H$ is also unexpected. While both $\Delta_{re}H$ and $\Delta_{va}H$ show (the same) a negative temperature dependence, the self-consistency of the reorientation model would require mutually opposite trends, since reorientiation of the host molecules may be regarded as partial desorption of these molecules, and this process is to some extent opposite to the (partial) adsorption of the guest molecules (Figure 8). One can speculate that the above contradictions can be resolved by inferring a pronounced cooperativity of intermolecular interactions between neighboring adsorbate molecules. In this way, however, we again arrive at the picture of surface aggregation, which holds for the half-cylindrical concept without internal inconsistency and with more thermodynamic arguments. We may conclude, therefore, that our results are consistent with the formation of half-cylindrical hemimicelles, as proposed by Manne et al., and are not congruent with the earlier reorientation model. It is desirable to extend this study to closely related systems to gain further insight into the thermodynamics of the adsorption of ionic surfactants from aqueous solutions on hydrophobic substrates.

Conclusions

The simultaneous measurement of the adsorption isotherm and the calorimetric enthalpies of displacement proved to be a sensitive method for elucidating the adsorption/aggregation behavior of surfactants at the solid/solution interface. Displacement of water (2) by C_{12}TAB (1) at the graphite surface proceeds in two distinctive stages with increasing surfactant concentration. The first stage of the displacement process is strongly exothermic and is *apparently* independent of the temperature (in the range from 288 to 318 K) and the surface coverage. The second stage of the displacement is less exothermic than the first, and it is not or only weakly dependent on the surface coverage. This second stage is further characterized by a strong, negative temperature dependence. The results of the thermodynamic analysis are consistent with the formation of a horizontally adsorbed surfactant monolayer, followed by the formation of half-cylindrical interfacial aggregates, as proposed in a recent AFM study. The earlier reorientation concept, i.e., a gradual change from a horizontal to a vertical orientation, accompanied by the adsorption of further incoming molecules, is not supported by the present results.

Acknowledgment. Z. K. thanks the Alexander von Humboldt Foundation for a research fellowship. This work was partially supported by the Deutsche Forschungsgemeinschaft (SFB 193) and OTKA (T025002).

Supporting Information Available: Numerical data of the adsorption isotherms and the calorimetric enthalpy isotherms of displacement (2 pages). Ordering information is given on any current masthead page.

References and Notes

(1) Denoyel, R.; Rouquerol, F.; Rouquerol, J. In *Adsorption from Solution*; Ottewill, R. H., Rochester, C. H., Eds.; Academic: London, 1983; p 225.
(2) Partyka, S.; Zaini, S.; Lindheimer, M.; Brun, B. *Colloids Surf.* **1984**, *12*, 255.
(3) Gellan, A.; Rochester, C. H. *J. Chem. Soc., Faraday Trans. 1* **1985**, *81*, 3109.
(4) Partyka, S.; Lindheimer, M.; Zaini, S.; Keh, E.; Brun, B. *Langmuir* **1986**, *2*, 101.
(5) Denoyel, R.; Rouquerol, F.; Rouquerol, J. In *Proceedings of the 2nd Engineering Foundation Conference on Fundamentals of Adsorption* (Santa Barbara, California, May 4−9, 1986); Liapis, A. I., Ed.; Am. Inst. Chem. Eng.: New York, 1987; p 199.
(6) Noll, L. A. *Colloids Surf.* **1987**, *26*, 43.
(7) Thomas, F.; Bottero, J. Y.; Partyka, S.; Cot, D. *Thermochim. Acta* **1987**, *122*, 197.
(8) Lindheimer, M.; Keh, E.; Zaini, S.; Partyka, S. *J. Colloid Interface Sci.* **1990**, *138*, 83.
(9) Denoyel, R.; Rouquerol, J. *J. Colloid Interface Sci.* **1991**, *143*, 555.
(10) Partyka, S.; Lindheimer, M.; Faucompre, B. *Colloids Surf. A* **1993**, *76*, 267.
(11) Giordano, F.; Denoyel, R.; Rouquerol, J. *Colloids Surf.* **1993**, *71*, 293.
(12) Giordano-Palmino, F.; Denoyel, R.; Rouquerol, J. *J. Colloid Interface Sci.* **1994**, *165*, 82.
(13) Seidel, J.; Wittrock, C.; Kohler, H.-H. *Langmuir* **1996**, *12*, 5557.
(14) Király, Z.; Börner, R. H. K.; Findenegg, G. H. *Langmuir* **1997**, *13*, 3308.
(15) Noll, L. A. *Calorim. Anal. Therm.* **1985**, *16*, 12.
(16) van Os, N. M.; Haandrikman, G. *Langmuir* **1987**, *3*, 1051.
(17) Seidel, J. *Thermochim. Acta* **1993**, *229*, 257.
(18) Woodbury, G. W., Jr.; Noll, L. A. *Colloids Surf.* **1988**, *33*, 301.
(19) Denoyel, R.; Rouquerol, F.; Rouquerol, J. *Colloids Surf.* **1989**, *37*, 295.
(20) Partyka, S.; Keh, E.; Lindheimer, M.; Groszek, A. *Colloids Surf.* **1989**, *37*, 309.
(21) Seidel, J. *Prog. Colloid Polym. Sci.* **1992**, *89*, 176.
(22) Sivakumar, A.; Somasundaran, P.; Thach, S. *J. Colloid Interface Sci.* **1993**, *159*, 481.
(23) Mehrian, T.; de Keizer, A.; Korteweg, A. J.; Lyklema, J. *Colloids Surf. A* **1993**, *73*, 133.
(24) Trompette, J. L.; Zajac, J.; Keh, E.; Partyka, S. *Langmuir* **1994**, *10*, 812.
(25) Lyklema, J. *Prog. Colloid Polym. Sci.* **1994**, *95*, 91.
(26) Corkill, M. J.; Goodman, J. F.; Tate, J. R. *Trans. Faraday Soc.* **1966**, *62*, 979.
(27) Corkill, M. J.; Goodman, J. F.; Tate, J. R. *Trans. Faraday Soc.* **1967**, *63*, 2264.
(28) Hey, M. J.; MacTaggart, J.; Rochester, C. H. *J. Chem. Soc., Faraday Trans. 1* **1984**, *80*, 699.
(29) Gellan, A.; Rochester, C. H. *J. Chem. Soc., Faraday Trans. 1* **1985**, *81*, 1503.
(30) Findenegg, G. H.; Pasucha, B.; Strunk, H. *Colloids Surf.* **1989**, *37*, 223.
(31) Iyer, S. R. S.; Zettlemoyer, A. C.; Narayan, K. S. *J. Phys. Chem.* **1963**, *67*, 2112.
(32) Zettlemoyer, A. C.; Skewis, J. D.; Chessick, J. *J. Am. Oil Chem. Soc.* **1962**, *39*, 280.
(33) Zettlemoyer, A. C. *J. Colloid Interface Sci.* **1968**, *28*, 343.
(34) Manne, S.; Cleveland, J. P.; Gaub, H. E.; Stucky, G. D.; Hansma, P. K. *Langmuir* **1994**, *10*, 4409.
(35) Manne, S.; Gaub, H. E. *Science*, **1995**, *270*, 1480.
(36) Wanless, E. J.; Ducker, W. A. *J. Phys. Chem.* **1996**, *100*, 3207.
(37) Corrin, M. L.; Lind, E. L.; Roginsky, A.; Harkins, W. D. *J. Colloid Interface Sci.* **1949**, *4*, 485.
(38) Fava, A.; Eyring, H. *J. Phys. Chem.* **1956**, *60*, 890.
(39) Vold, R. D.; Sivaramakrishnan, N. H. *J. Phys. Chem.* **1958**, *62*, 984.
(40) Saleeb, F. Z.; Kitchener, J. A. *J. Chem. Soc.* **1965**, 911.
(41) Day, R. E.; Greenwood, F. G.; Parfitt, G. D. In *Proceedings of the 4th International Congress on Surface Active Substances* (Brussels,

September 7−12, 1964); Overbeek, J. Th. G., Ed.; Gordon & Beach: New York, 1967; p 1005.
(42) Connor, P.; Ottewill, R. H. *J. Colloid Interface Sci.* **1971**, *37*, 642.
(43) Ma, C.; Xia, Y. *Colloids Surf.* **1992**, *66*, 215.
(44) Gabrielli, G.; Cantale, F.; Guarini, G. G. T. *Colloids Surf.* **1996**, *119*, 163.
(45) Greenwood, F. G.; Parfitt, G. D.; Picton, N. H.; Wharton, D. D. In *Adsorption from Aqueous Solutions*; Weber, W. J., Matijevic, E., Eds.; American Chemical Society: Washington, DC, 1968; p 135.
(46) Groszek, A. J.; Partyka, S. *Langmuir* **1993**, *9*, 2721.
(47) Wang, H. L.; Duda, J. L.; Radke, C. J. *J. Colloid Interface Sci.* **1978**, *66*, 153.
(48) Koch, C. S.; Köster, F.; Findenegg, G. H. *J. Chromatogr.* **1987**, *406*, 257.
(49) Suurkuusk, J.; Wadsö, I. *Chem. Scr.* **1982**, *20*, 155.
(50) Woodbury, G. W.; Noll, L. A. *Colloids Surf.* **1987**, *28*, 233.
(51) Király, Z.; Dékány, I. *Prog. Colloid Polym. Sci.* **1990**, *83*, 68.
(52) Liphard, M.; Glanz, P.; Pilarski, G.; Findenegg, G. H. *Prog. Colloid Polym. Sci.* **1980**, *67*, 131.
(53) Király, Z.; Dékány, I.; Klumpp, E.; Lewandowski, H.; Narres, H. D.; Schwuger, M. J. *Langmuir* **1996**, *12*, 423.
(54) Denoyel, R.; Rouquerol, F.; Rouquerol, J. *J. Colloid Interface Sci.* **1990**, *136*, 375.
(55) Király, Z.; Dékány, I. *Colloid Polym. Sci.* **1988**, *266*, 663.
(56) Rasch, R.; Neumann, J.; de Keizer, A.; Király, Z.; Findenegg, G. H. To be published.
(57) Király, Z.; Findenegg, G. H. To be published.
(58) McGonigal, G. C.; Bernhardt, R. H.; Thomson, D. J. *Appl. Phys. Lett.* **1990**, *57*, 28.
(59) Rabe, P. J.; Buchholz, S. *Science* **1991**, *253*, 424.
(60) Groszek, A. J. *Proc. R. Soc. London* **1970**, *A134*, 473.
(61) Iwamoto, K.; Ohnuki, Y.; Sawada, K.; Seno, M. *Mol. Cryst. Liq. Cryst.* **1981**, *73*, 95.
(62) Barry, B. W.; Wilson, R. *Colloid Polym. Sci.* **1978**, *256*, 251.
(63) Pauling, L. *The Nature of the Chemical Bond*; Cornell University: Ithaca, NY, 1960; p 261.
(64) Bury, R.; Mayaffre, A.; Treiner, C. *J. Chem. Soc., Faraday Trans. 1* **1983**, *79*, 2517.
(65) Bergström, S.; Olofsson, G. *Thermochim. Acta* **1986**, *109*, 155.
(66) Ozeki, S.; Ikeda, S. *J. Colloid Interface Sci.* **1982**, *87*, 424.
(67) Imae, T.; Ikeda, S. *J. Phys. Chem.* **1986**, *90*, 5216.
(68) Imae, T.; Kamiya, R.; Ikeda, S. *J. Colloid Interface Sci.* **1985**, *108*, 215.
(69) Reiss-Husson, F.; Luzzati, V. *J. Phys. Chem.* **1964**, *68*, 3504.
(70) Malliaris, A.; Le Moigne, J.; Sturm, J.; Zana, R. *J. Phys. Chem.* **1985**, *89*, 2709.
(71) Bashford, M. T.; Woolley, E. M. *J. Phys. Chem.* **1985**, *89*, 3173.
(72) Dearden, L. V.; Woolley, E. M. *J. Phys. Chem.* **1987**, *91*, 4123.
(73) Woolley, E. M.; Bashford, M. T. *J. Phys. Chem.* **1986**, *90*, 3039.
(74) Missel, P. J.; Mazer, N. A.; Benedek, G. B.; Young, C. Y.; Carey, M. C. *J. Phys. Chem.* **1980**, *84*, 1044.
(75) Mazer, N. A.; Olofsson, G. *J. Phys. Chem.* **1982**, *86*, 4584.
(76) Bach, J.; Blandamer, M. J.; Bijma, K.; Engberts, J. B. F. N.; Kooreman, P. A.; Kacperska, A.; Rao, K. C.; Subha, M. C. S. *J. Chem. Soc., Faraday Trans.* **1995**, *91*, 1229.